MECHANIKA TEORETYCZNA
I STOSOWANA
Journal of Theoretical
and Applied Mechanics
2, 30, 1992

INVESTIGATION OF THERMAL STRESSES IN THE I BEAMS WITH CIRCULAR HOLES IN THE WEB

ZBIGNIEW ORŁOŚ

GRZEGORZ GALIN

Military Technical Academy, Warsaw

An experimental investigation of transient thermal stresses in the I beams with circular holes in the web is described. The experiments were performed using four photoelastic models of the I beams made of epoxy resin. The experiments reported in this paper included two–dimensional photothermoelastic analysis, measurements of thermal strains and transient temperature distributions. The results of experimental investigations enabled Authors to propose the computational FEM model for the analysis of transient thermal stresses in the webs of the I beams models.

1. Introduction

In recent years thermal–stresses problems have been of considerable interest. These problems are of great importance in the design of airplanes, jet engines and nuclear reactors. In this paper we shall consider the nature and magnitude of the transient thermal stresses in the I beams with circular holes in the web. The experimental techniques that create a photoelastic model of a thermal load similar to the load of the actual object have been investigated. The material used for the models was Araldite B. The thermal stresses in the web were measured photoelastically and compared to the values computed numerically by the finite element techniques. Various experimental techniques were used to simulate the desired temperature gradients and to observe the resulting stresses [1,2,3].

The tests presented here were conducted on equipment and according to a testing technique which were specifically developed to simplify photothermoelastic studies under transient conditions. The technique of cooling by using powdered dry ice has been adopted.

2. Experimental procedure

The geometry of the models made of Araldite B photoelastic material is shown in Fig.1.[1] The temperature dependent mechanical, thermal and photoelastic properties of the material were measured before the tests. Over the range of temperatures from 200° K to 290° K the photoelastic figure of merit $Q_t = 17.5$ fringe/mK remained nearly constant.

The upper surface of the flange of the I beam model was uniformly and suddenly cooled. The temperature at selected points in the model was monitored with the aid of fine copper–constantan thermocouples cemented into the model with epoxy resin. The thermovision technique was used to determine the isotermal lines. Electrical–resistance strain gages were used for measuring thermal strains of the upper surface of the flange.

Standard two–dimensional photoelastic techniques were used to determine the isoclinics and isochromatics on the web of the model. The diffused light polariscope with 500 mm diameter field size was used. Diagrammatic layout of experimental equipment is shown in Fig.2. Continuous temperature measurement was performed, and simaltaneously the photoelastic fringes were photographed and registred using television recording.

3. Results and conclusions

In this experiment the Biot number is defined as

$$\mathrm{Bi} = \frac{hH}{k} \tag{3.1}$$

where

h – convective–heat–transfer coefficient,

k – thermal conductivity,

H – height of the beams.

The convective–heat–transfer coefficient was determined by measuring the temperature distribution over a special test beam made of epoxy resin. The experiments on I beam models resulted in an effective Biot number of 190 ± 10.

In Fig.3 is shown the dark–field isochromatic fringe pattern in the web of the "200" model at the time 30, 120 and 600 s after the thermal loading. Fig.4 shows the fringe order N distributions along the contour of the hole at 120 and 600 s. Along the free boundary the tangential stress is a principal one. For the models

[1] cf the end of the paper

used in the investigation reported here the nondimensional stress σ^* can be written as

$$\sigma^* = \frac{N}{Q_t g(T_0 - T_z)} \tag{3.2}$$

where

- N – photoelastic–fringe order on the free boundary,
- g – thickness of the web,
- T_0 – ambient temperature; i.e., the initial temperature of the model,
- T_z – temperature of the powdered dry ice.

The thermal strains of the upper surface of the flange were measured by the applied rosette strain gages and recorded. The computed thermal stresses σ_ξ parallel to the longitudal direction of the flange and the thermal stresses σ_η in the width direction are given in Fig.5 as the functions of time t after thermal loading.

The transient thermal stresses in the I beams models were determined using finite element analysis. A detail of the finite element mesh of the "200" model is shown in Fig.6. The experimental results agree well with the theoretical ones.

The distributions of temperature and the stresses σ_x in the symmetrical section of the "200" model are presented in Fig.7 and 8. The comparison of experimental and theoretical temperature distributions along the axis of symmetry of the cross section of the "100" model is shown in Fig.9.

The main results obtained are summarized as follows.

The upper surface of the cooled flange of the I beam model was subject to a state of two–dimensional thermal stresses. The maximum thermal stresses in this surface of the flange occur at 5 s after the thermal loading.

In the present investigation of webs containing the holes the maximum thermal stress occured at the edge of hole located near the cooled flange.

The results of numerical computations using the finite element technique are seen to be in good agreement with the measured values of stresses in all four models.

References

1. IWAKI T., MIYAO K., *Transient Thermal Stresses in a Strip with an Eccentric Hole,* Experimental Mechanics, **24**, 1984, 22-27

2. IWAKI T., *Transient Thermal Stresses in Fully and Partly Cooled Circular Rings,* Experimental Mechanics, **26**, 1986, 163-168

3. HIRAI N, SAITO A., *Photothermoelastic Measurements by Means of High Frequency Induction Heating Apparatus,* Journal of Thermal Stresses, **6**, 1983, 153-165

Badanie naprężeń cieplnych w belkach dwuteowych z okrągłymi otworami w środniku

Streszczenie

W pracy przedstawiono opis badań doświadczalnych naprężeń cieplnych w belkach dwuteowych z okrągłymi otworami w środniku. Badania przeprowadzono na czterech modelach belek dwuteowych, które wykonano z żywicy epoksydowej. Przedstawione doświadczenia obejmują zarówno dwuwymiarową analizę termoelastooptyczną, pomiary naprężeń cieplnych jak i rozkłady temperatury. Wyniki badań doświadczalnych wykorzystano do zaproponowania modelu obliczeniowego opartego na MES umożliwiającego analizę elastooptycznych naprężeń cieplnych w środnikach modeli belek dwuteowych.

Praca wpłynęła do Redakcji dnia 19 września 1990 roku

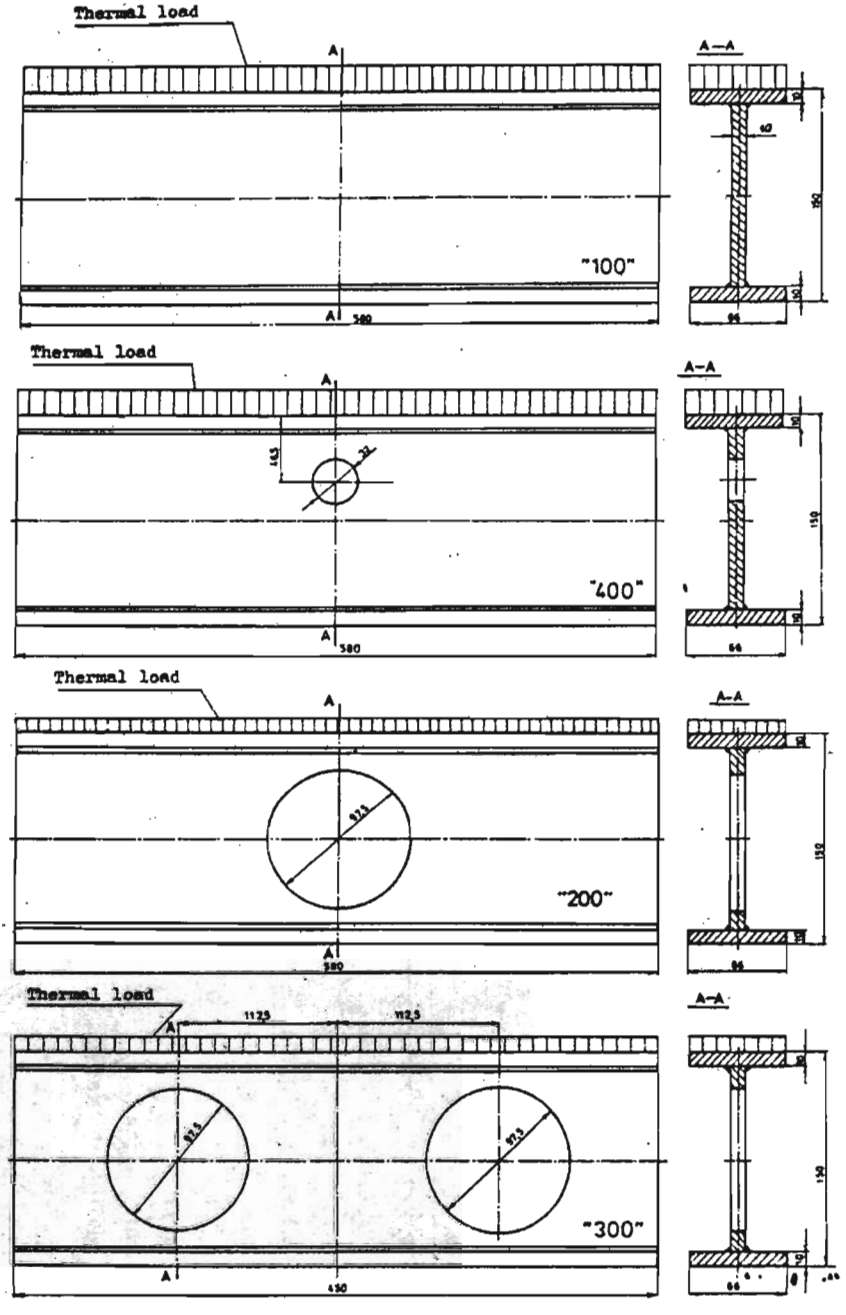

Fig. 1. Geometry of the photoelastic I beam models

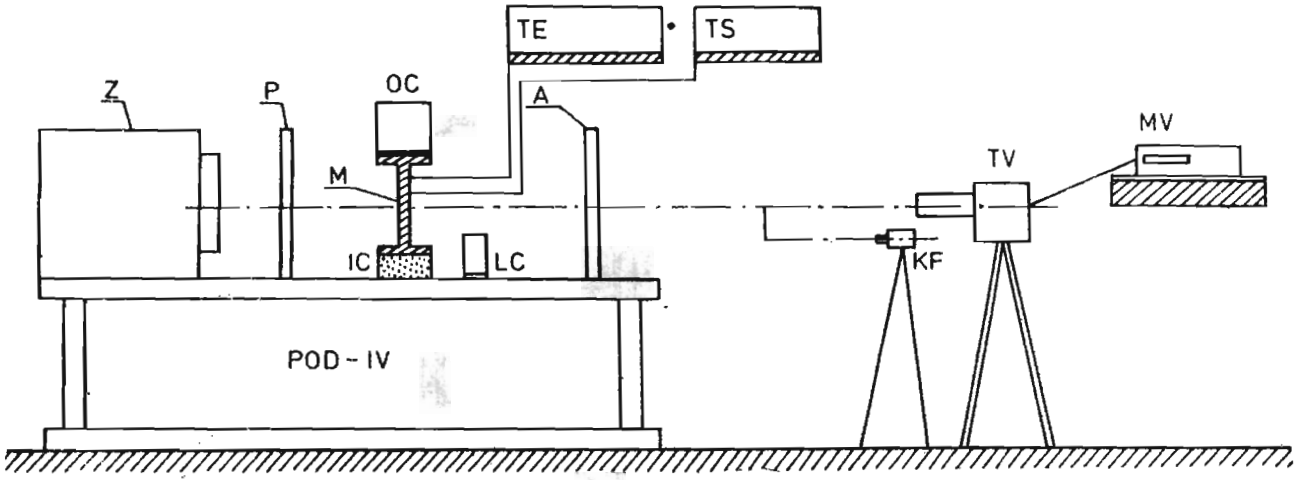

Fig. 2. The experimental setup

Z	–	white and monochromatic light source	TE	–	multi–point recorder of temperature
P	–	polarizer	TV	–	television camera
A	–	analyzer	MV	–	video tape recorder
M	–	model	LC	–	time meter
OC	–	thermal load	KF	–	camera
IC	–	thermal insulation	TS	–	automatic multi–channel strain gages recording system

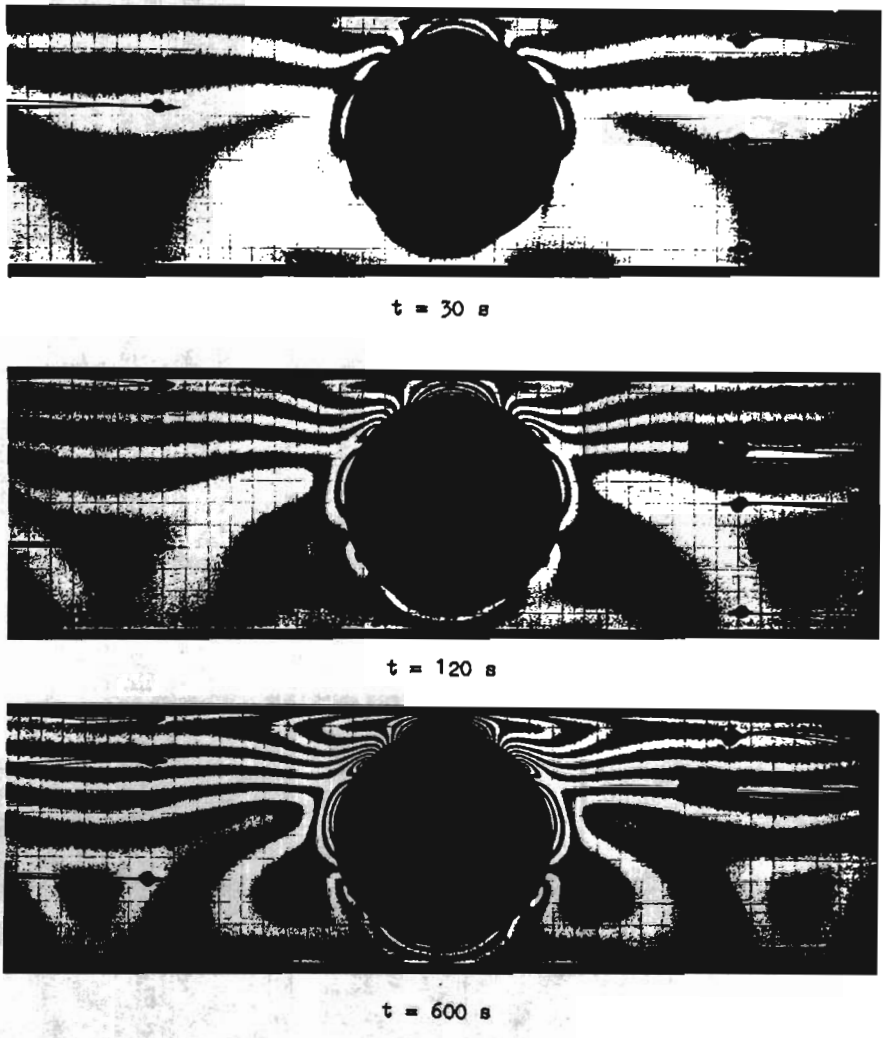

Fig. 3. Dark–field isochromatic fringes in the web of the model "200" at time 30, 120 and 600 s

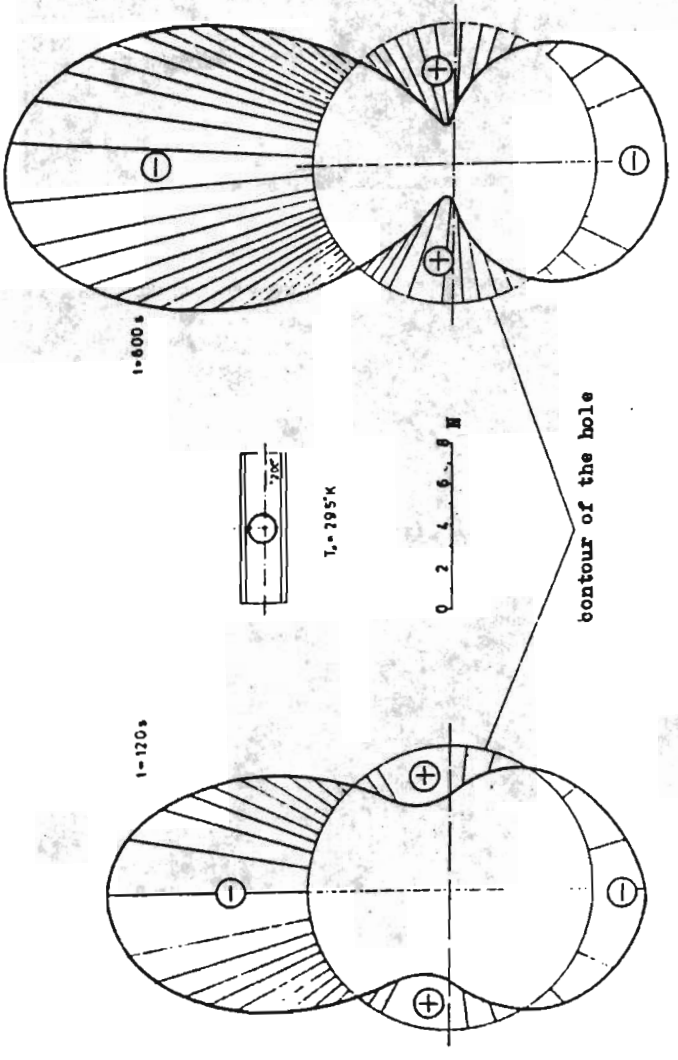

Fig. 4. Photoelastic fringe order N distributions along the contour of the hole (Fig.3) at time 120 and 600 s

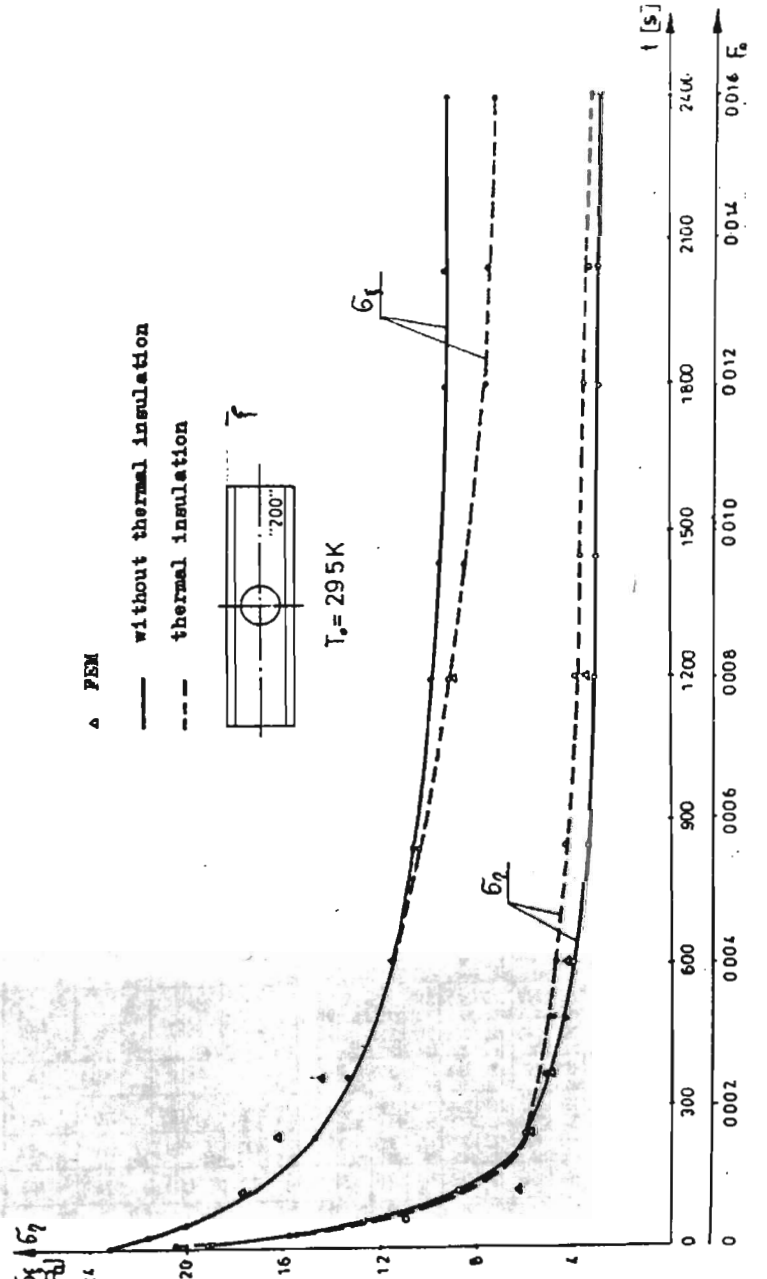

Fig. 5. Thermal stresses σ_ξ and σ_η as the function of time t

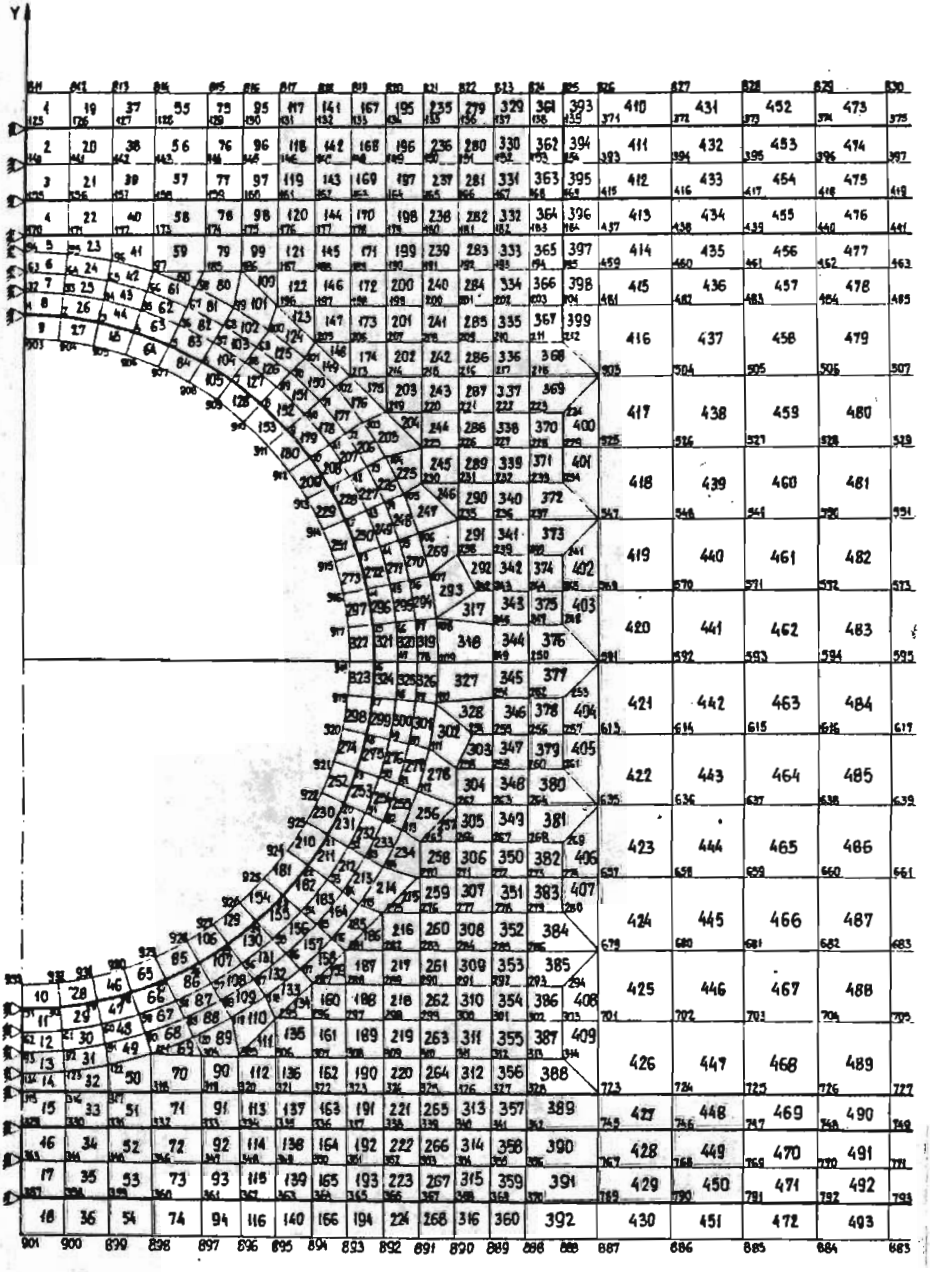

Fig. 6. A detail of the finite element mesh of the "200" model

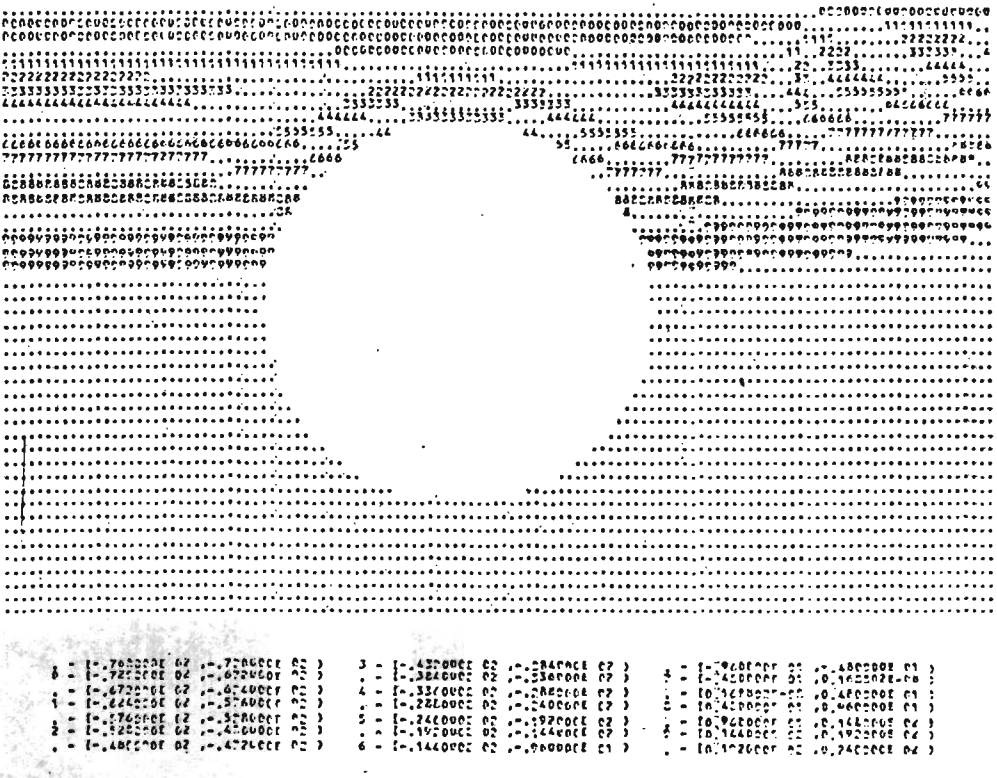

Fig. 7. Distribution of temperature in the half of the "300" model at 2400 s

– for optical patterns, observed on the reflection

$$\rho = L\sqrt{2N\frac{\lambda}{W}} \tag{3.15}$$

– for optical patterns, observed in transmission in accordance with the results of paper [23].

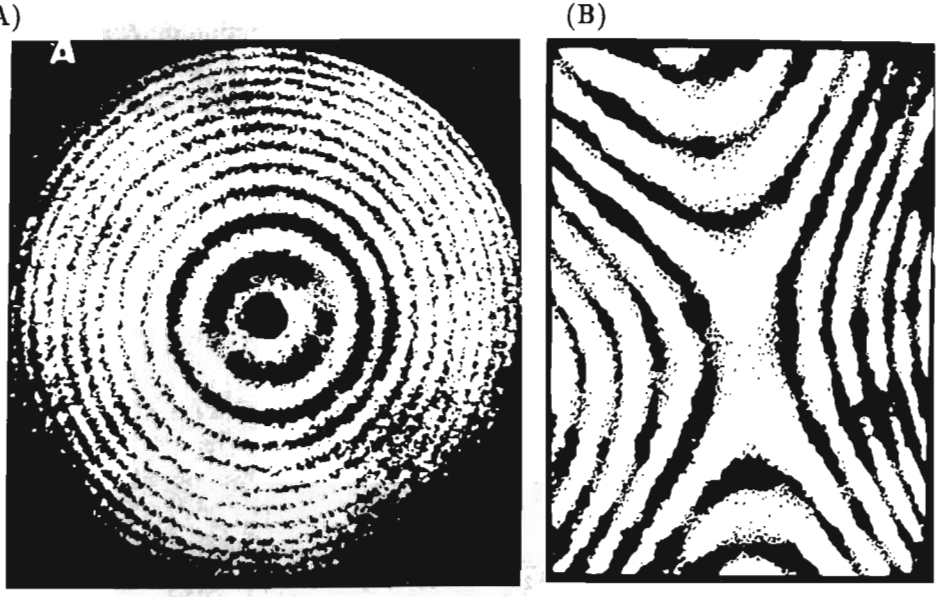

Fig. 7. Photographs of the interference fringes for displace ment W = const: A – displacement of a sample as a rigid body, B – one–axis axial extension of a plane sample

It follows from Eq (3.13) that $W = 2(L/\rho)(\lambda L/a)$.

This function completely coincides with the previously obtained as a result of the experiment described earlier by the Author [24] and by Chiang F.P., et al. [25] (coefficient 2 on the right–hand side of the formula appeared due to the double path of the beams between the sample and the holographic plate in the diagram of hologram recordings, done in opposed beams).

The most frequently used interferential and optical methods are employed when we solve plane elasticity and plasticity problems.

Let us assume, that the strains of a axially loaded thin strip are examined in the direction of axis $\hat{x}$ with the help of the superimposed interferometer. The origin of the coordinate system $\hat{x}\hat{y}\hat{z}$ rigidly connected to the sample surface coincides with the fixed point of the holographic plate on the sample surface, the axes $\hat{x}, x, x_1, x_2$ have the similar directions.

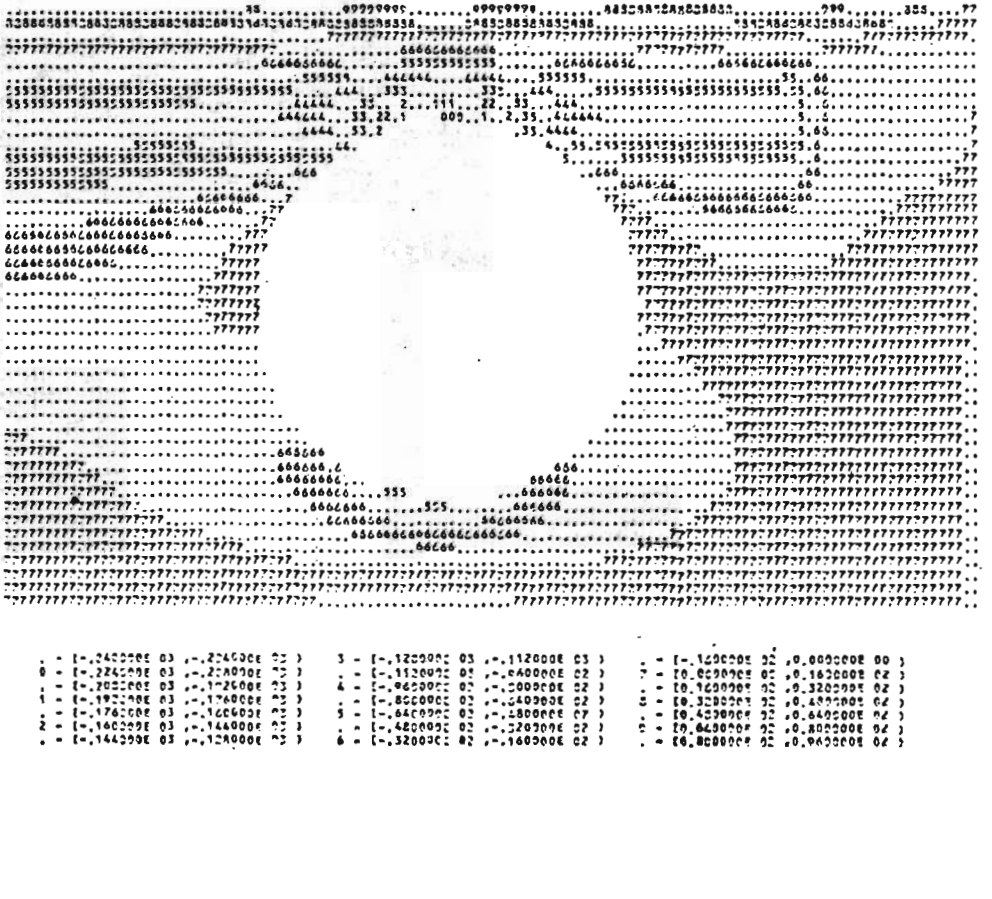

Fig. 8. Distribution of stress σ_z in the half of the "300" model at time 600 s

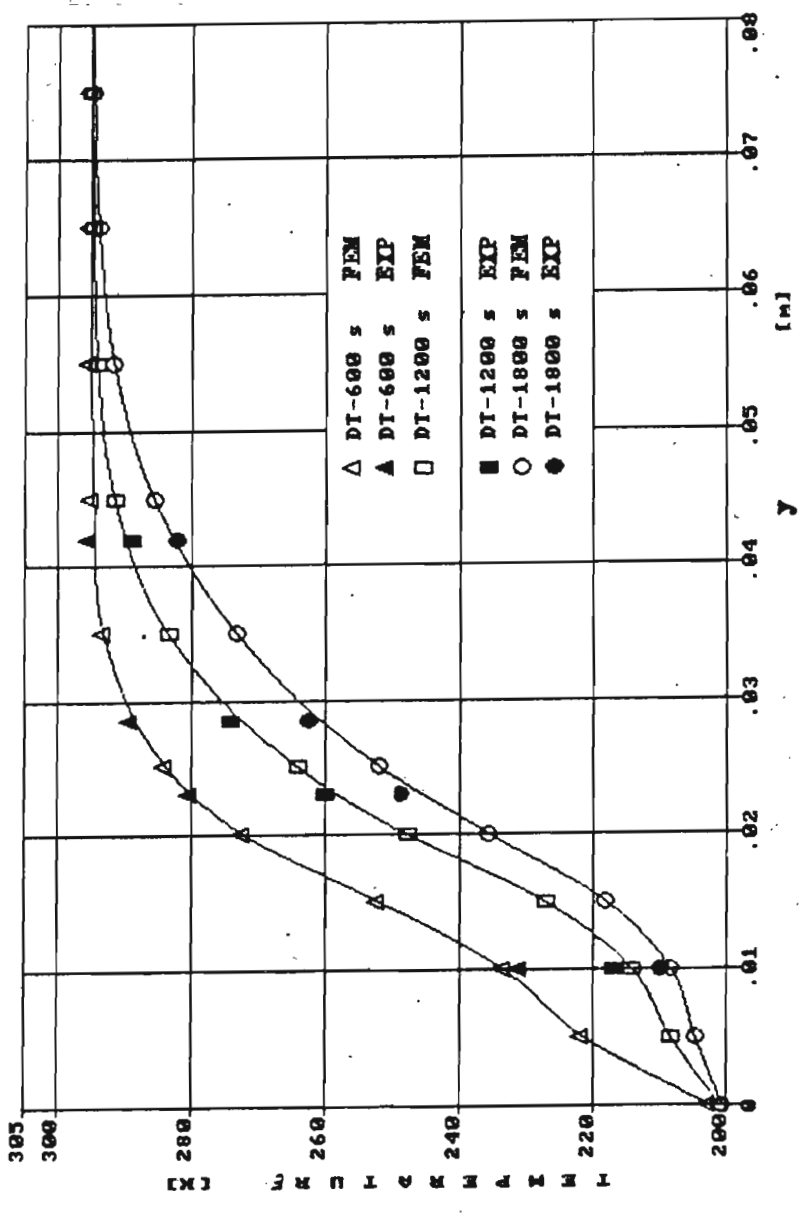

Fig. 9. Experimental and theoretical temperature distributions along the axis of symmetry of the cross-section of the "100" model (y – distance from the upper surface of the flange)